Evaluation of CT injection to RFP for performance improvement and reconnection studies

S. Masamune

A. Sanpei, T. Nagano, S. Nakanobo, R. Tsuboi, S. Kunita, M. Emori, H. Makizawa, H. Himura, N. Mizuguchi[1] , T. Akiyama[1], T. Mizuuchi[2], K.J. McCollam[3], D.J. Den Hartog[3], R. Paccagnella[4]

Kyoto Institute of Technology, Kyoto 606-8585, Japan
[1] *NIFS, Toki 509-5292 , Japan*
[2] *Inst. Adv. Energy, Kyoto University, Uji, Japan*
[3] *University of Wisconsin-Madison, WI 53706, USA*
[4] *Consorzio RFX, Padova 32157, Italy*

US-Japan CT2016 Workshop, Aug 22-24, Irvine, CA

Outline

- Motivation of low-A RFP research
- RELAX machine and its operational region
- QSH state in RELAX with 3-D MHD simulations
- MHD feedback control and performance improvement
- Gas fueling and helicity injection for further performance improvement
- Relaxation and magnetic reconnection
- Summary

Motivation to explore the low-aspect-ratio RFP - I

- **Resonant/non-resonant mode numbers depend on *A*.**
- **Lower n (m=1) mode becomes resonant as *A* is lowered.**

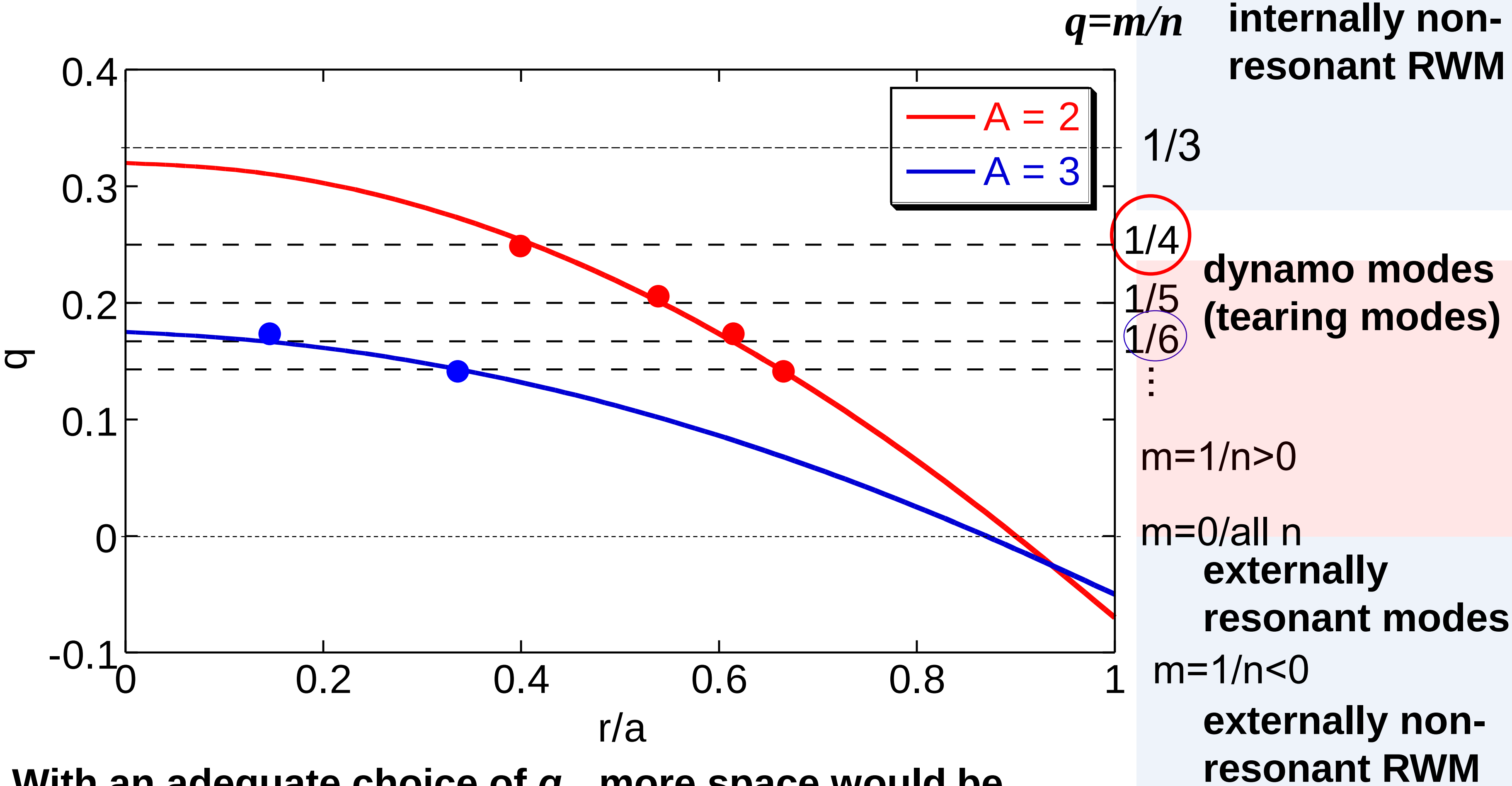

With an adequate choice of q_0, more space would be available in the core region without major resonant surface

Motivation to explore low-A RFP - II

Bootstrap current fraction is sensitive to *A* and pressure profiles

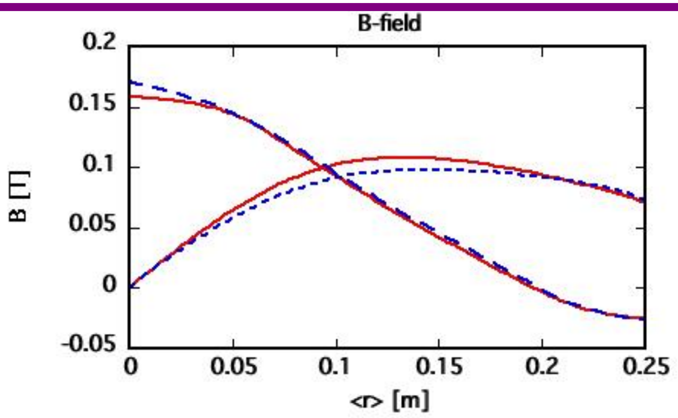

- Sizable bootstrap current could be expected in low-*A* RFP (with very high-beta). (Shiina, 2005)
- Estimate of the bootstrap current fraction with equilibrium reconstruction using "RELAXFit" shows:

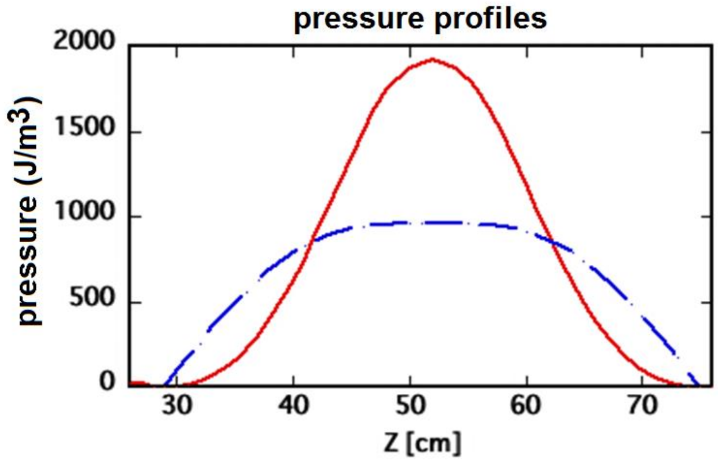

- Peaked pressure profile with rather flat temperature profile
- **$T_e(0)$=300 eV, $n_e(0)=4.0\times10^{19}\ m^{-3}$ at I_p=90 kA (n_G~1.0)**
- poloidal beta =24%

  => bootstrap current fraction ~ 30%

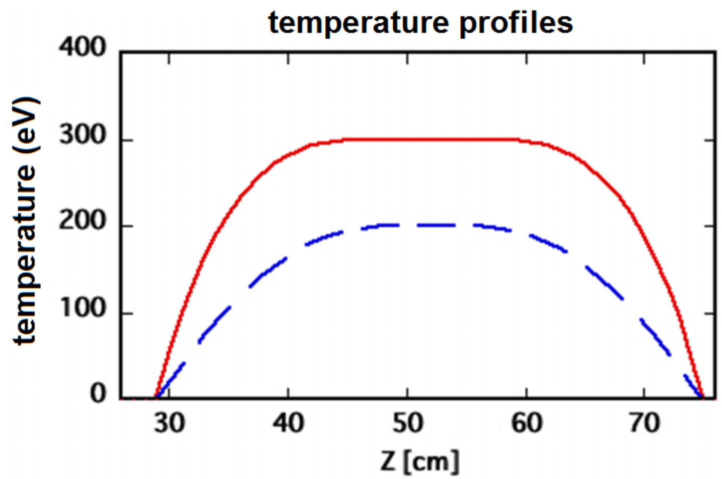

- Flat profiles for both pressure and temperature
- **$T_e(0)$=200 eV, $n_e(0)=3\times10^{19}\ m^{-3}$ at I_p=95 kA**
- poloidal beta = 31%

  => bootstrap current fraction ~ 5%

REversed field pinch of Low-Aspect-ratio eXperiment

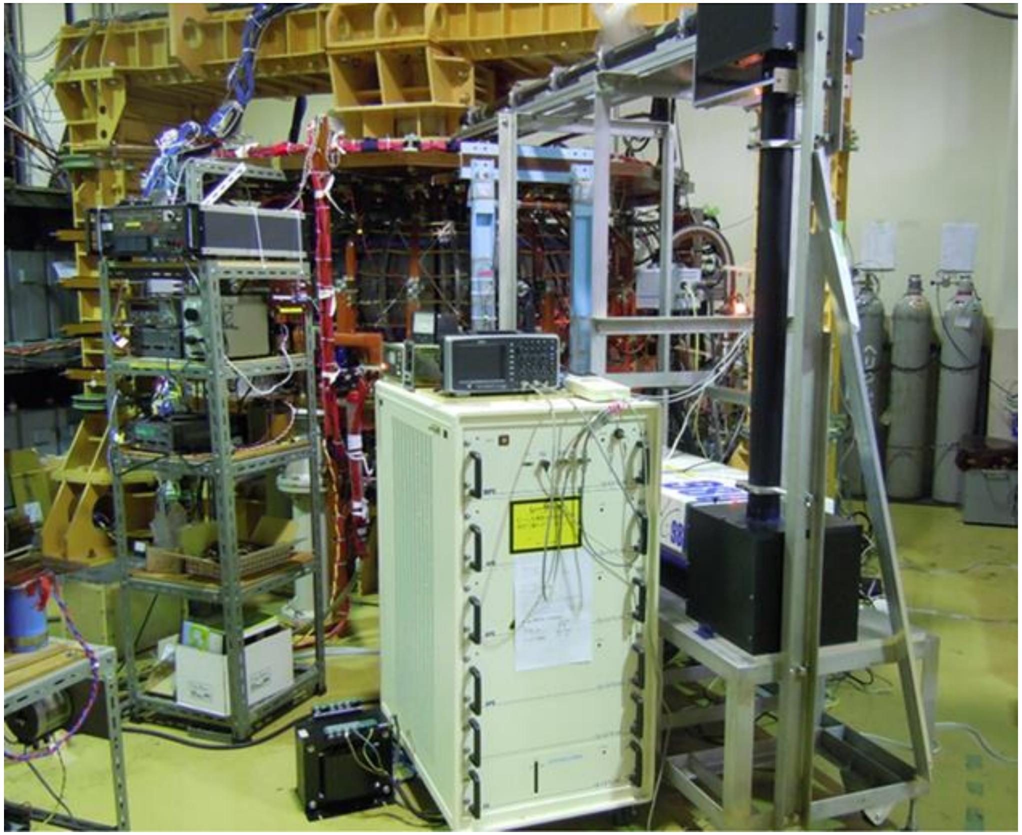

Kyoto Institute of Technology

Objectives of RELAX includes:
- geometrical optimization of RFP
- bootstrap current issues
- MHD with resistive wall boundary

$R/a = A = 2$
(0.51 m/0.25 m)

Resistive wall boundary

$I_p < 125$ kA
$n_e = 10^{18} \sim 2 \times 10^{19}$ m^{-3}
$T_e(0) \sim 100\text{-}200$ eV
$\beta_{pe0} \sim 5\text{-}15\%$
$\tau_D > 3$ ms

Wide operational range in (F, Θ) space is realized in RELAX

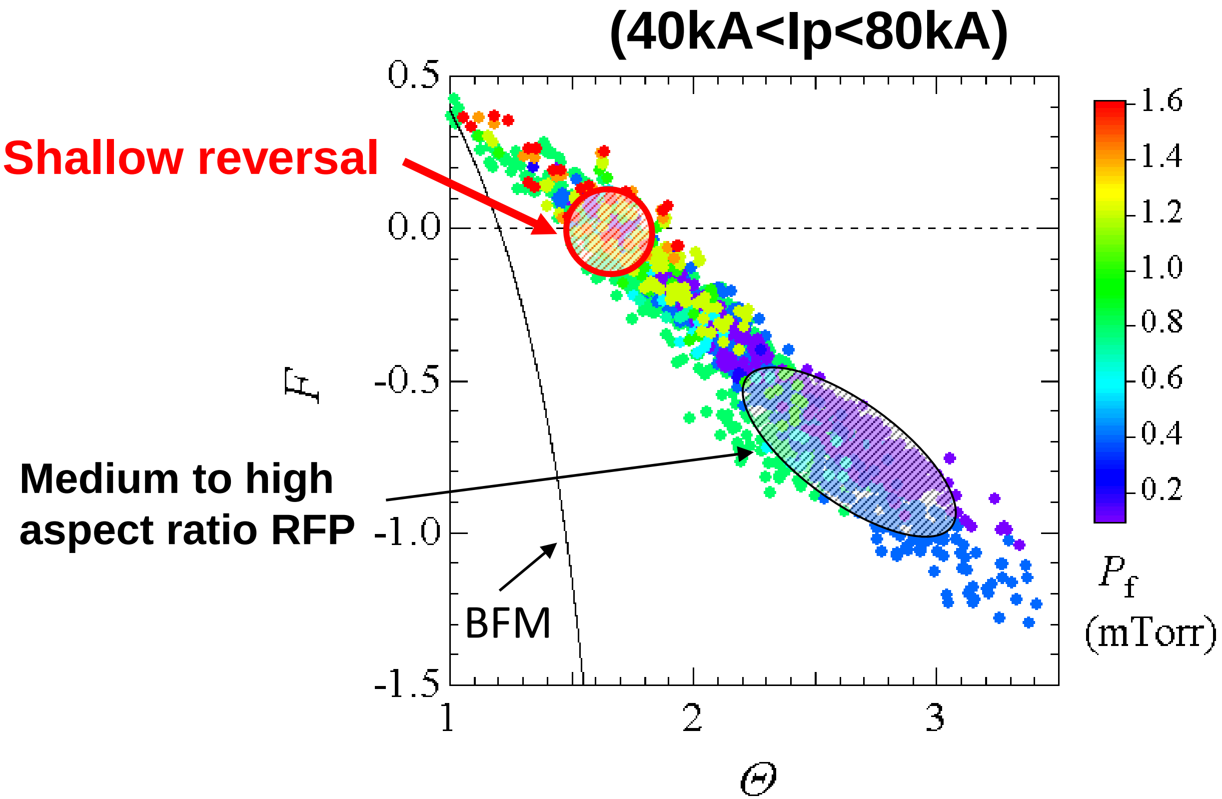

$$\Theta = \frac{B_p(a)}{\langle B_t \rangle}$$

$$F = \frac{B_t(a)}{\langle B_t \rangle}$$

(Ikezoe et al., PPCF 2012)

- **In shallow reversal region,**
  - **Periodic Quasi-Single Helicity (QSH) or Helical Ohmic RFP state tends to be realized**
- **In deep reversal, high-Θ region,**
  - **Amplitudes of resonant modes are suppressed with broad spectrum**
  - **SXR emission increases, indicating improved plasma performance**

Example of QSH in RELAX from edge magnetic fluctuation

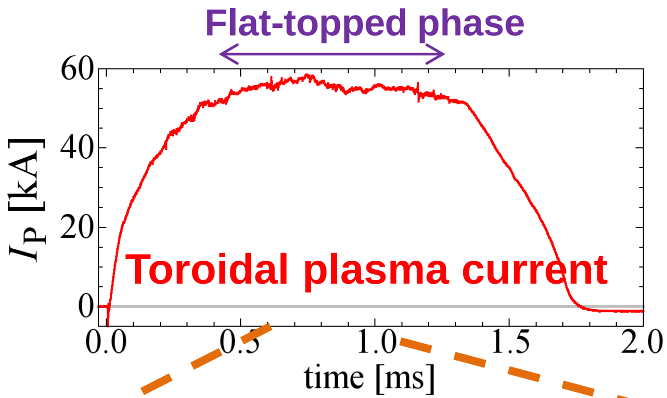

- QSH defined by $N_s<2$ can be confirmed from edge magnetic fluctuation spectrum.
- QSH appears quasi-periodically.

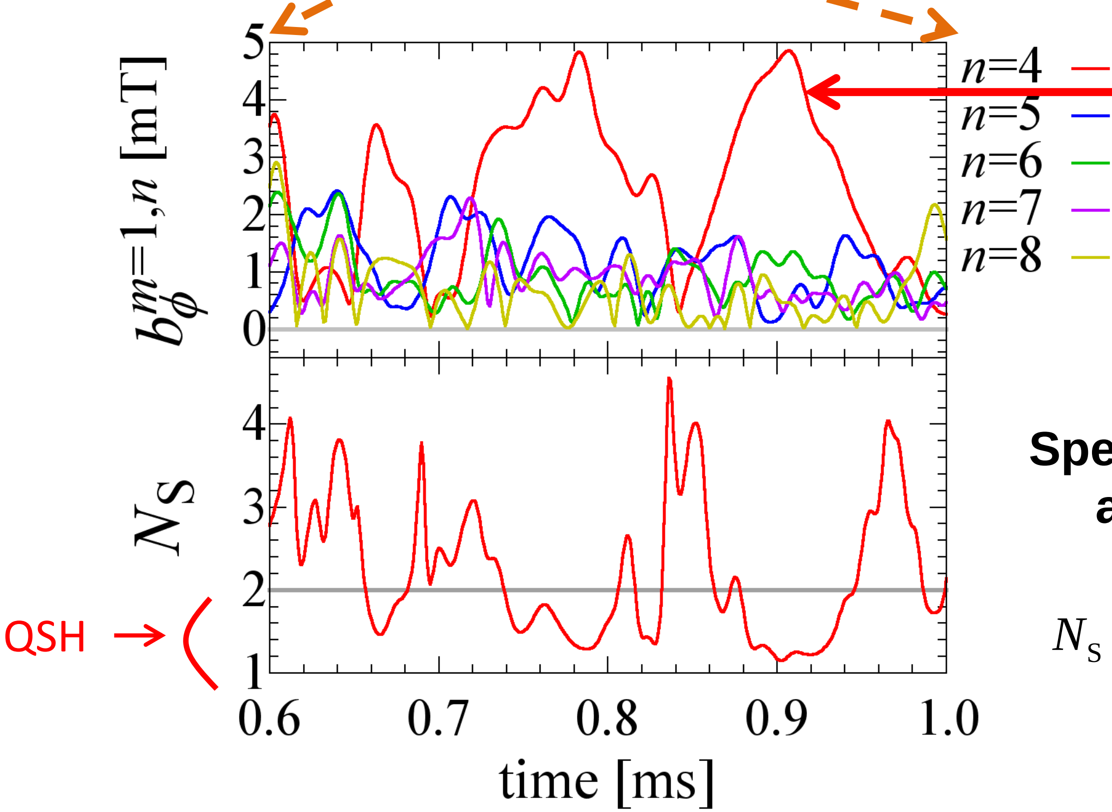

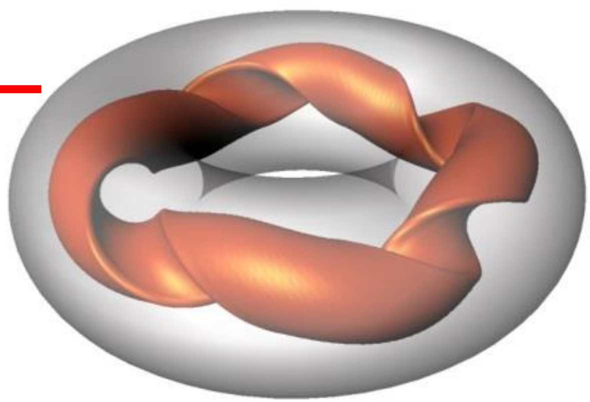

Spectral index Ns:
a quantitative measure for QSH

$$N_S = \left[\sum_{n=3}^{8} \left(\frac{\left(b_\phi^{1,n}\right)^2}{\sum_{n=3}^{8} \left(b_\phi^{1,n}\right)^2} \right)^2 \right]^{-1}$$

(Oki et al, PFR 2012; FST 2013)

Comparison of the experimental and computed flux surfaces

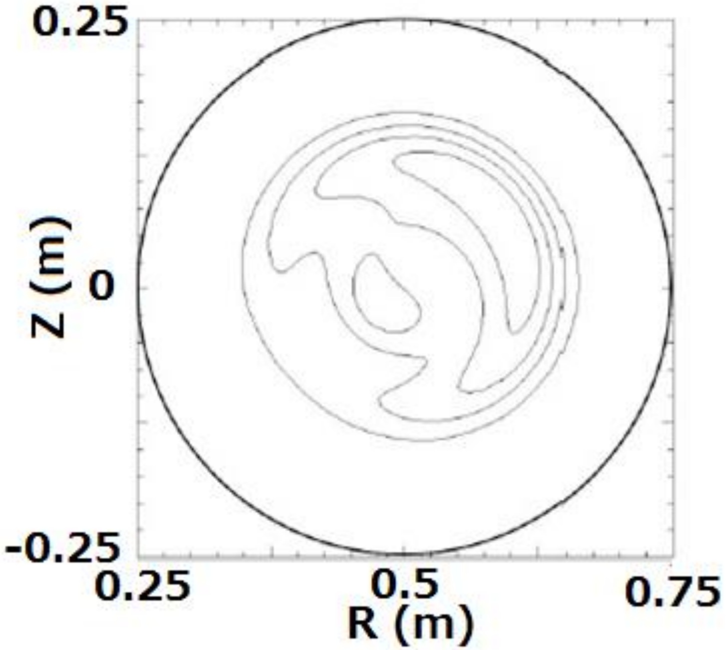

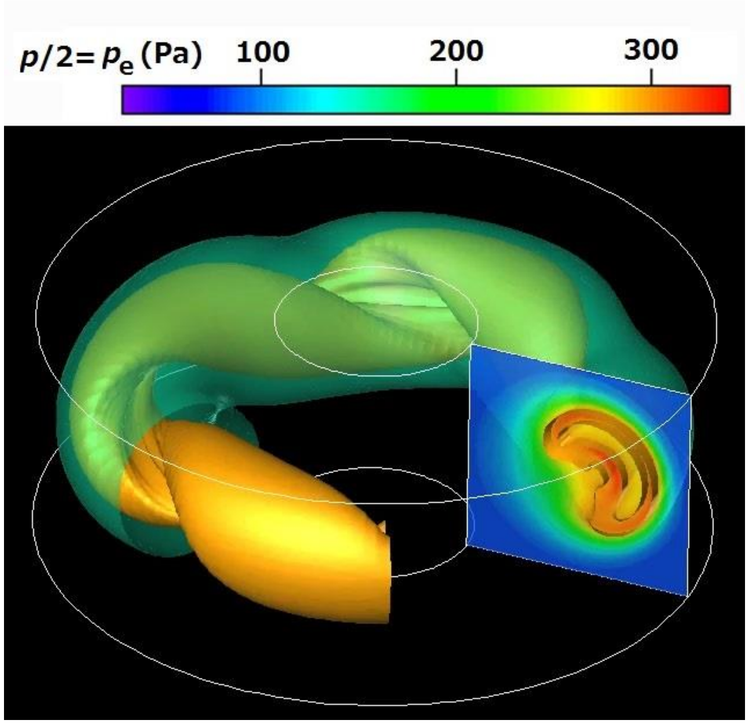

Left: reconstructed magnetic surface shape using SXR imaging and CT technique during QSH phase in RELAX. The major axis is to the left of the cross section. **Right**: helical equi-pressure surface shape in 3-D MHD simulation using the MIPS code. The helical states show good agreement.

Two processes are possible to form the helical core structure with resonant and non-resonant modes

Resonant case

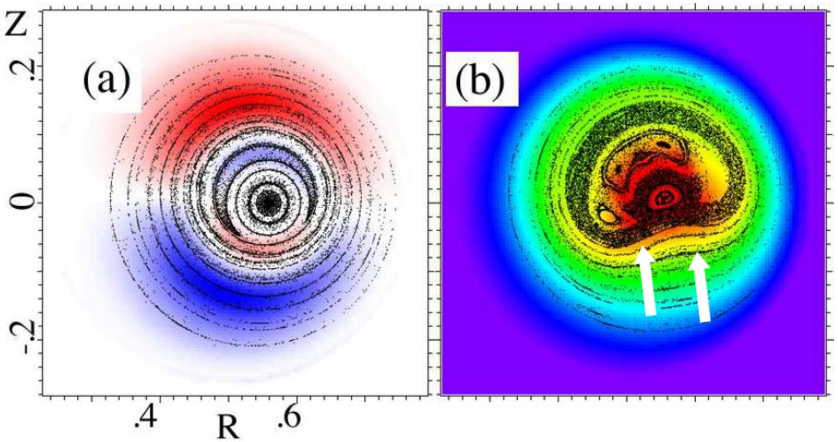

Non-resonant case

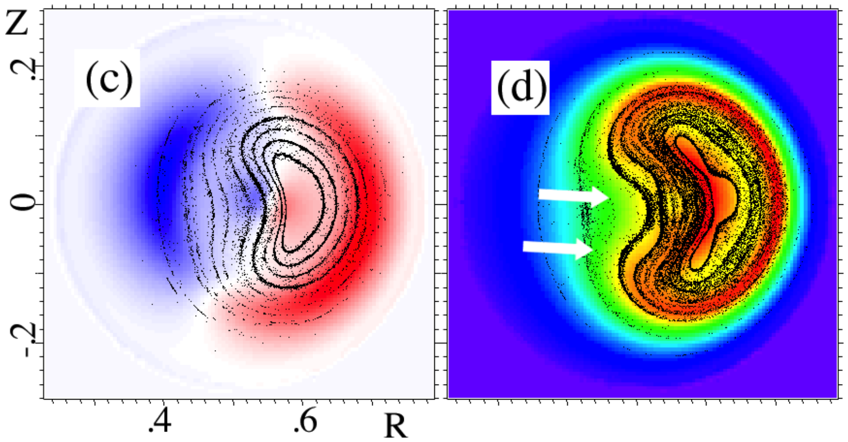

Resonant case

- **Magnetic island appears and grows on the q=1/4 surface, the original magnetic axis disappearing by helical flow-driven magnetic reconnection .**
- **The O-point of the island forms a new helical magnetic axis.**
- **A bean-shaped, hollow pressure profile is formed in a poloidal cross section**

Non-resonant case

- **The original magnetic surfaces deform directly into a helical shape.**
- **A bean-shaped, hollow pressure profile is still formed.**

(Mizuguchi et al., PPCF 2012)

Wide operational range in (*F*, *Θ*) space is realized in RELAX

(40 kA < I_p < 80kA)

Shallow reversal and non-reversed region

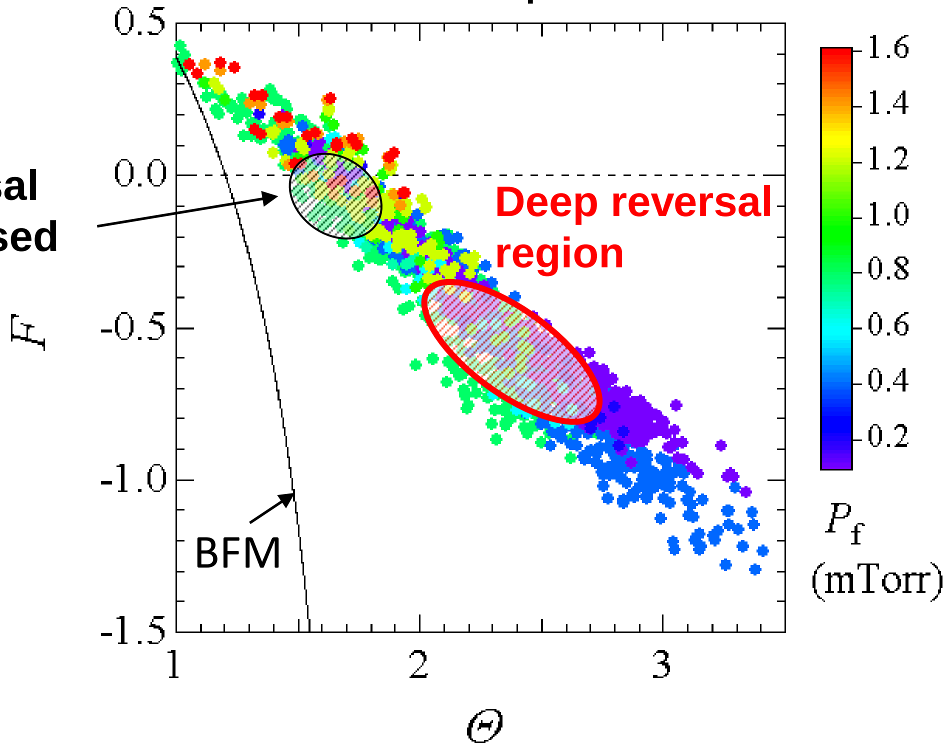

$$\Theta = \frac{B_p(a)}{\langle B_t \rangle}$$

$$F = \frac{B_t(a)}{\langle B_t \rangle}$$

(Ikezoe et al., PPCF 2012)

- **In shallow reversal region,**
  - **Quasi-periodic Quasi-Single Helicity (QSH) or Helical Ohmic RFP state tends to be realized**
- **In deep reversal, high-Θ region,**
  - **Amplitudes of resonant modes are suppressed with broad spectrum**
  - **SXR emission increases, indicating improved plasma performance**

The resistive wall mode in RELAX

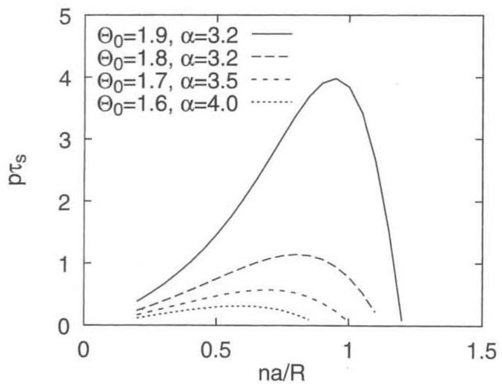

Fig. 3. Growth rate vs $ak_z = na/R$ for the equilibrium specified by four sets of Θ_0, α.

Linear stability analysis predicts the most unstable mode with nε~1, where ε=*a*/*R* (Masamune, 1998)

DEBS code simulation

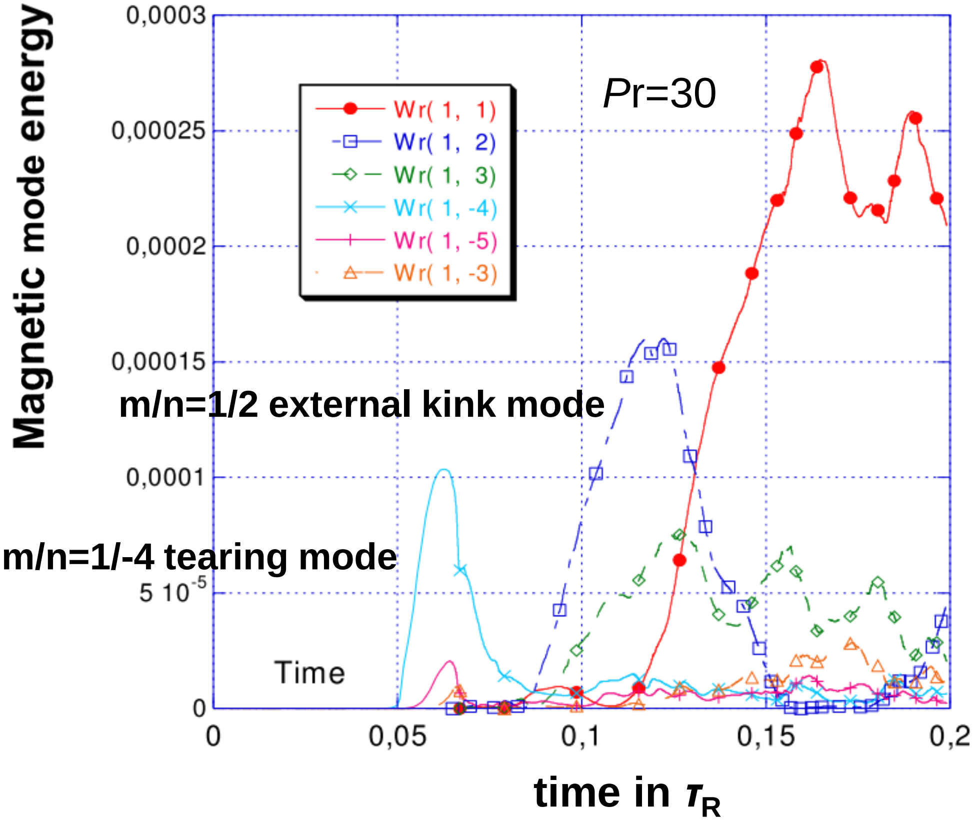

Radial mode energy vs. time for the RWM simulation with τ_w =0.02 (*Pr* = 30, *S* = 3x10^4) (Paccagnella, 2008)

Saddle coil array for feedback control of MHD modes

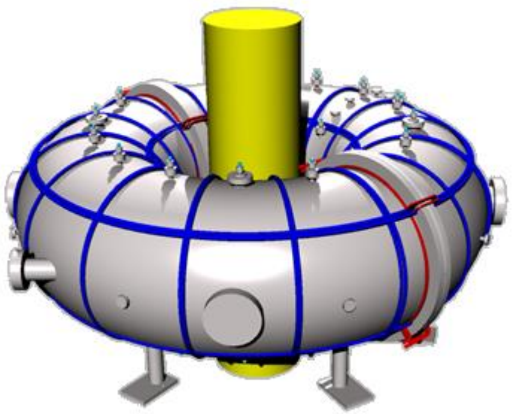

4x16 saddle coil array

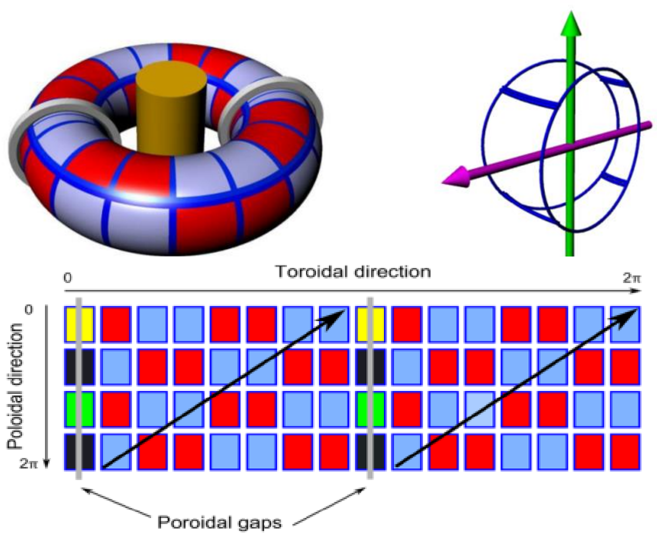

saddle coil connection for m/n=1/2 mode stabilization with separate control at two poloidal gaps

- **Feedback control of a single RWM has been performed using 64 saddle coils (4X16) covering the whole torus.**
- **The saddle coils are connected in series to form m/n=1/2 helical windings, with separate coils at two poloidal gaps, for stabilization of the most unstable RWM in RELAX.**

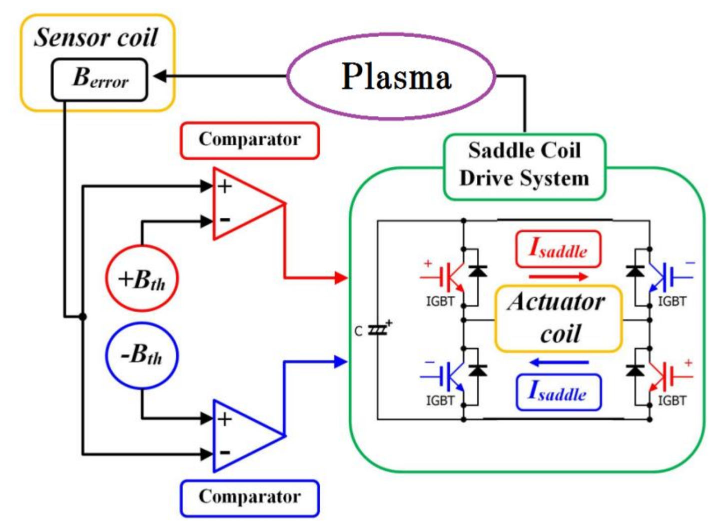

Diagram of the control power supply

Feedback control of single m/n=1/2 RWM has resulted in longer discharge duration (~ 3τ_w)

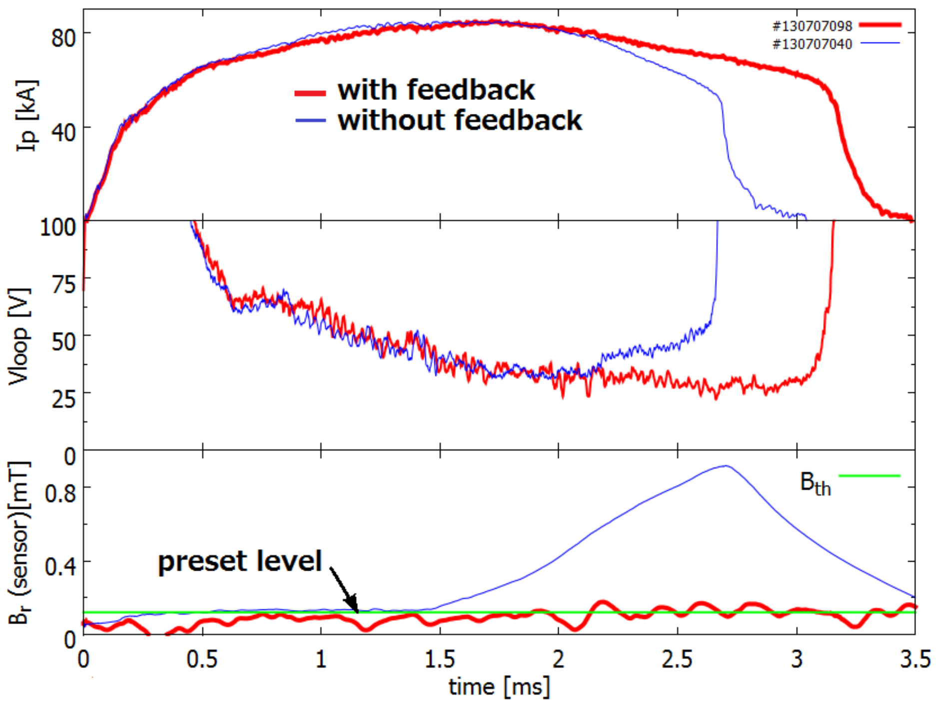

- **Feedback control of a single RWM has been performed using 64 saddle coils (4X16) covering the whole torus.**
- **As a result of feedback control, the sensor signals are suppressed below the pre-set level over the discharge**
- **The discharge duration extends to ~3ms, restricted by iron core saturation**

(Tanaka et al., PFR 2014)

Poloidal currents at the insulated gaps produce signals to the feedback sensor coils

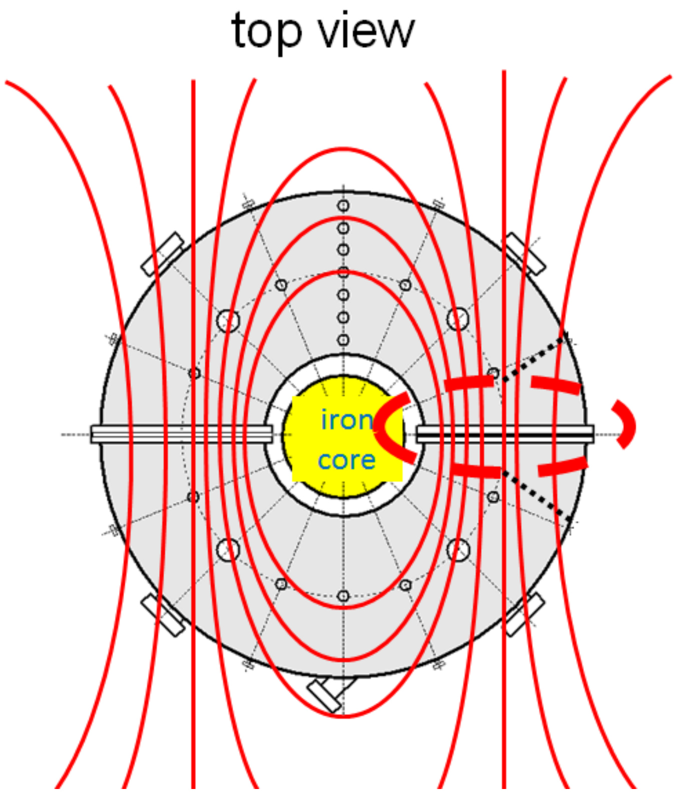

- ➢ **Poloidal current flows in the vessel and flanges when the reversed toroidal field is applied in the current rise phase.**
- ➢ **The poloidal current persists because of the longer L/R time of the flanges.**
- ➢ **The resultant fields produce signals to the feedback sensor coils as m/n=1/2 component.**

Independent control at the poloidal gaps leads to further improvement

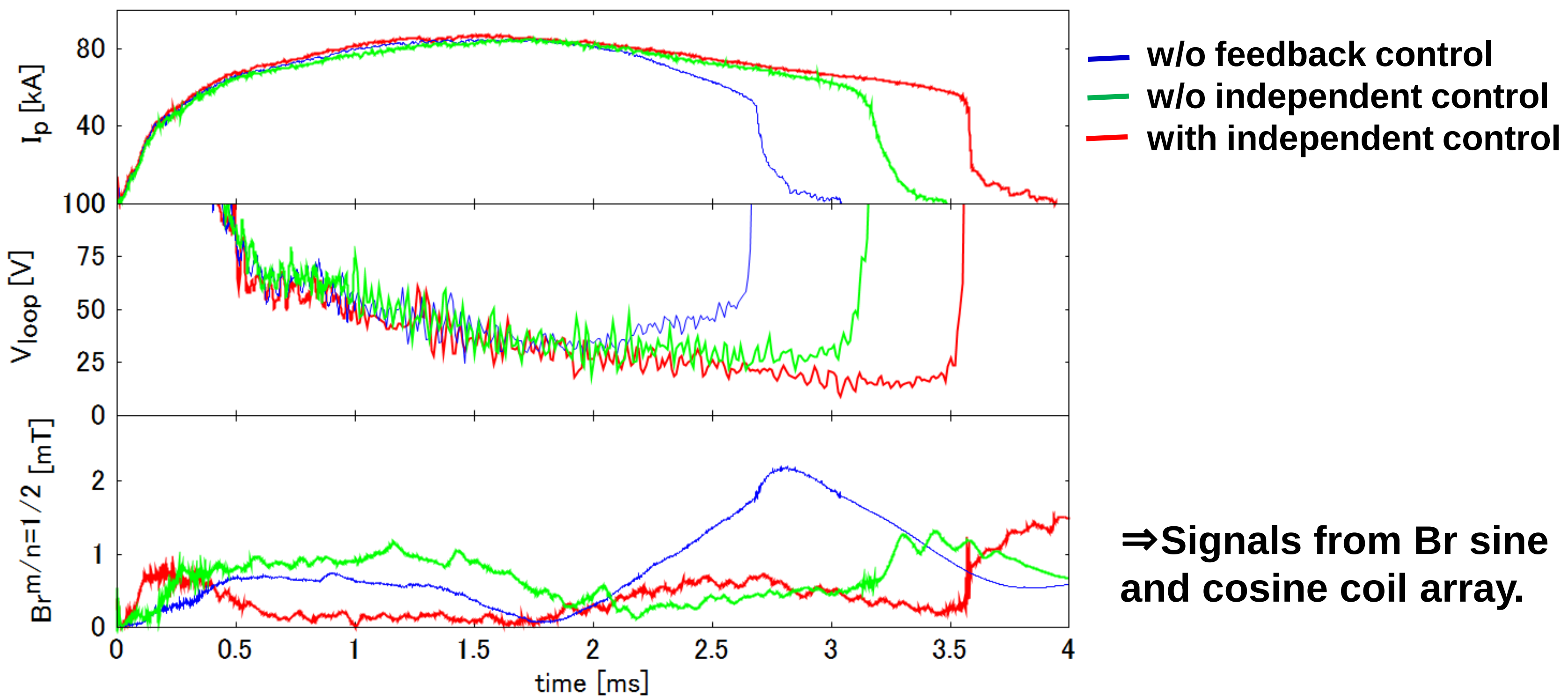

⇒Signals from Br sine and cosine coil array.

- **m/n=1/2 mode amplitude (outside the vessel) is lowered particularly during the current rise phase.**
- **In the three cases, the discharge duration is limited by the saturation of iron core (~0.2 Vs).**

Thomson temperature provides central electron pressure p_{e0}

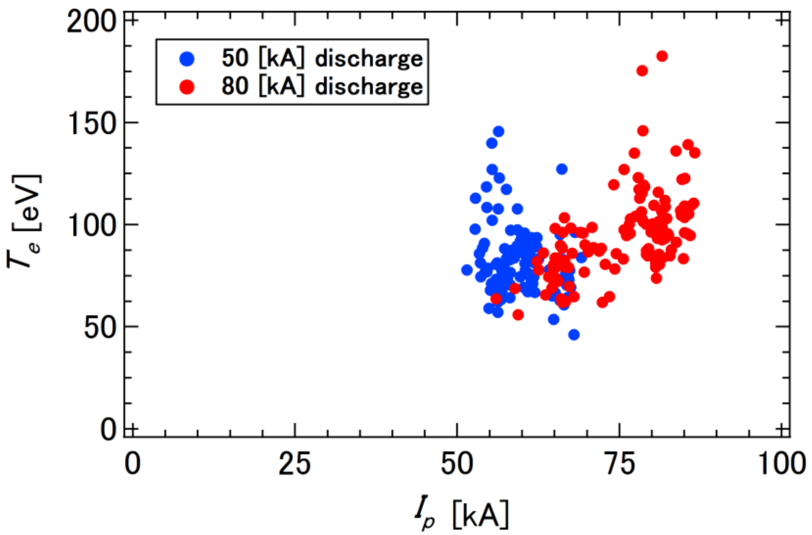

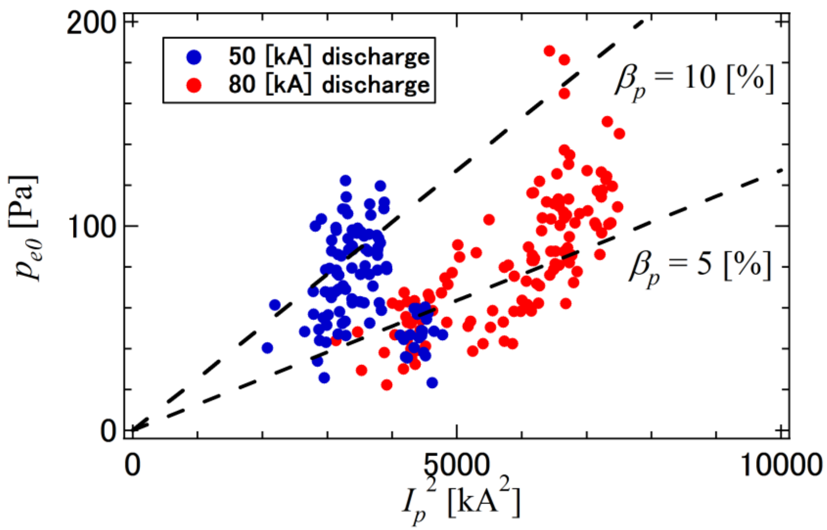

- **The central electron temperature Te(0) is ~100 eV for Ip of 50-80kA, is increasing with Ip.**
- **The maximum central electron pressure increases with plasma current.**
- **A measure of electron beta, $\beta_p \equiv p_{e0} / (B_p^{\ 2}(a) / 2\mu_0)$, is 5-15%.**

(Ueba et al., PFR 2014)

Density dependence on electron beta is under investigation

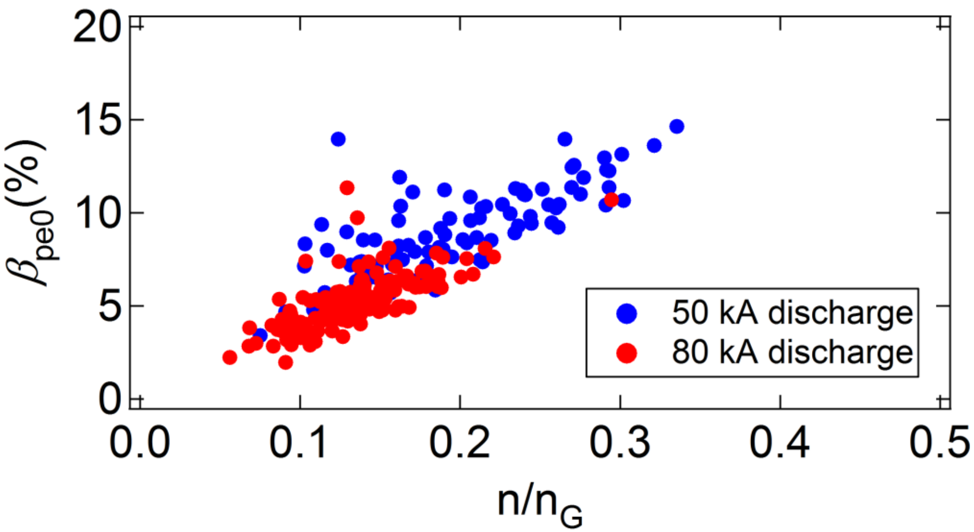

- **The electron beta increases with density well below the Greenwald density limit.**
- **The electron poloidal beta increases with density in the region below the Greenwald density.**
- **A 140 GHz millimeter wave interferometer is working.**
- **Preliminary gas injection experiment seems to be promising.**

Simple nozzle has been tested for directional gas flow

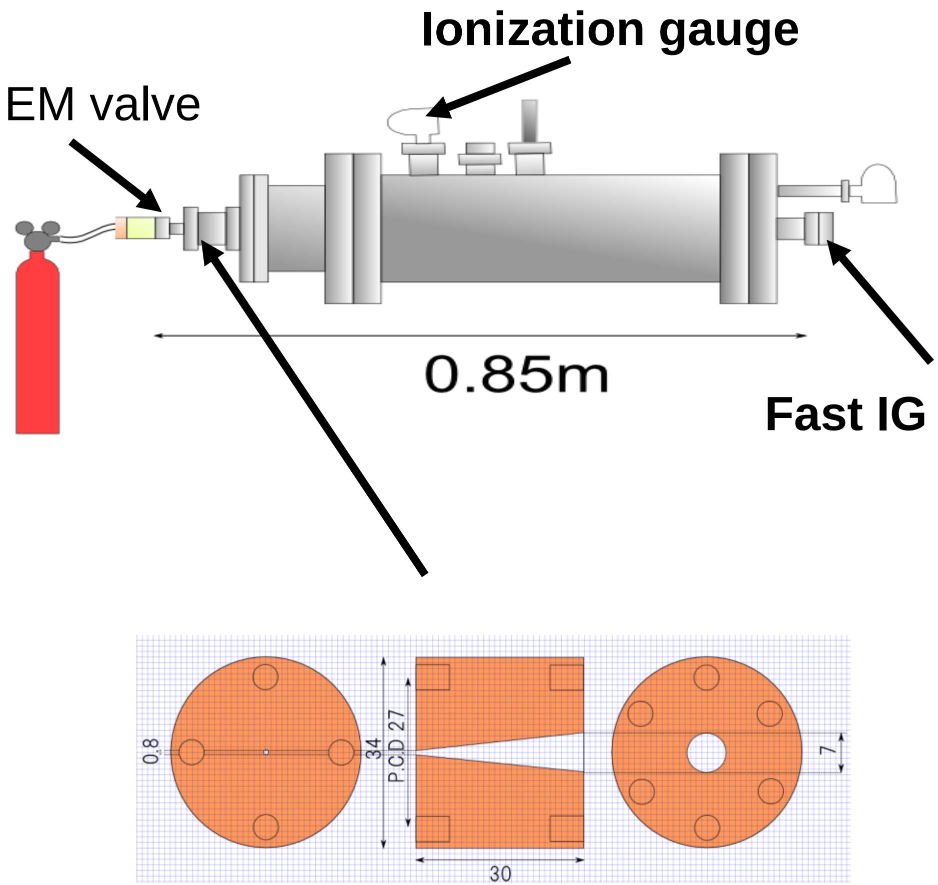

Simple nozzle

- **A simple nozzle has been tested in combination with fast acting electromagnetic valve**
- **Gas flow velocity is estimated using a fast ionization gauge facing the nozzle**

Directional gas flow at least v > 1km/s has been confirmed

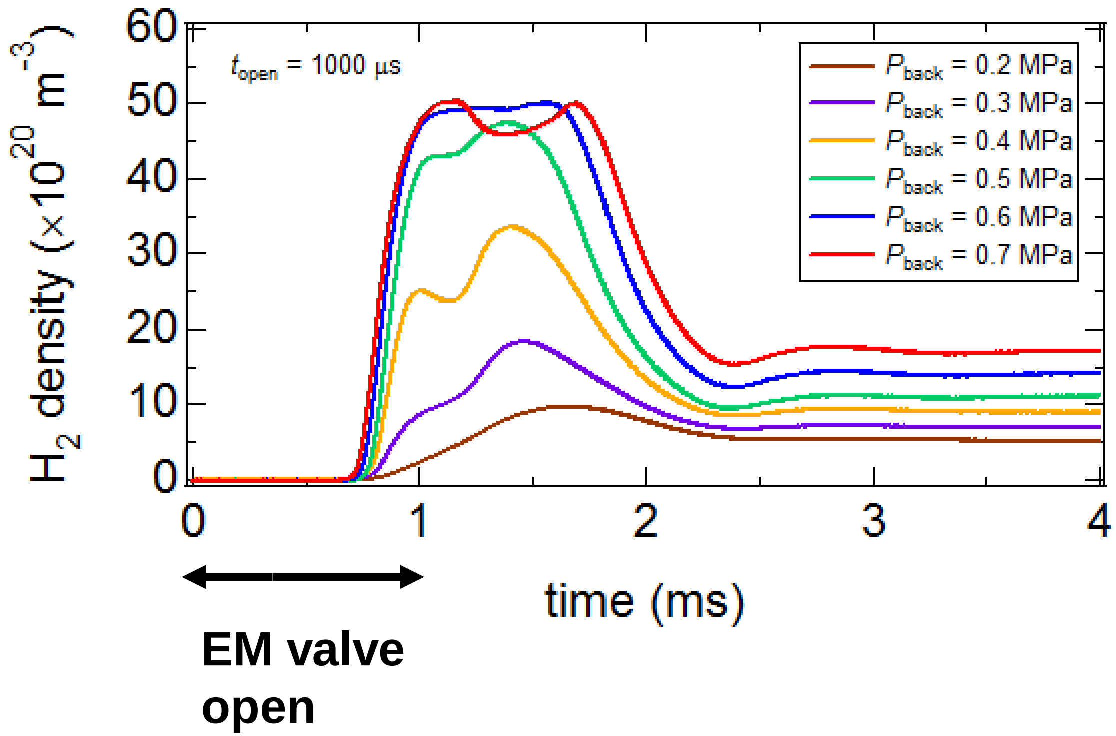

- **Initial rapid increase in pressure followed by decay to steady value may be an indication of directional gas flow**

- **The total number of injected H_2 particles can be estimated from steady state pressure**

Magnetic helicty in a toroidal system

$$K_1 = \int \boldsymbol{A} \cdot \boldsymbol{B} \, \mathrm{d}V - \Phi \Psi$$

$$\frac{dK_1}{dt} = -2 \int \boldsymbol{E} \cdot \boldsymbol{B} \, \mathrm{d}V - 2\dot{\Phi} \Psi - \int \nabla \cdot (\phi \boldsymbol{B}) \, \mathrm{d}V$$

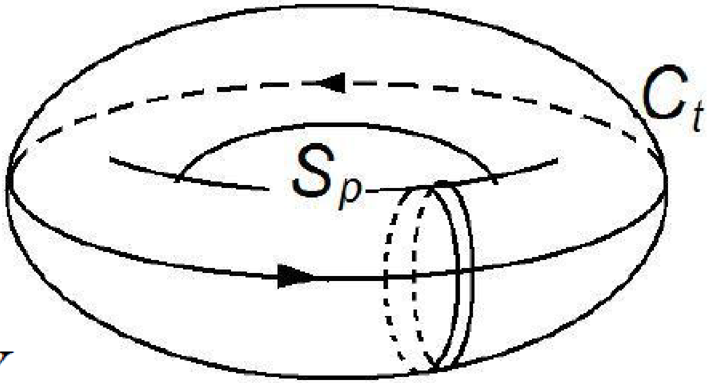

Magnetic helicity in RELAX plasma at Ip~100kA:

$$\Psi \approx 6 \times 10^{-3} \, (Wb)$$
$$\Phi \approx 0.1 \, (Wb)$$

$$\Rightarrow \quad K_1 \approx 6 \times 10^{-4} \, (Wb^2)$$

CT Injector for TPE-RX

The injector is transferred to RELAX

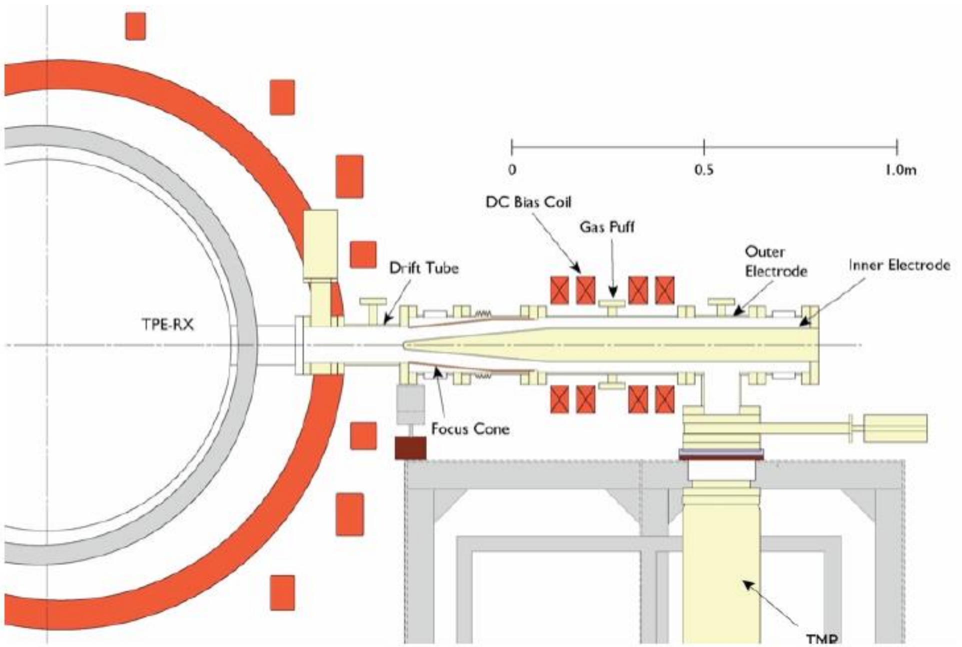

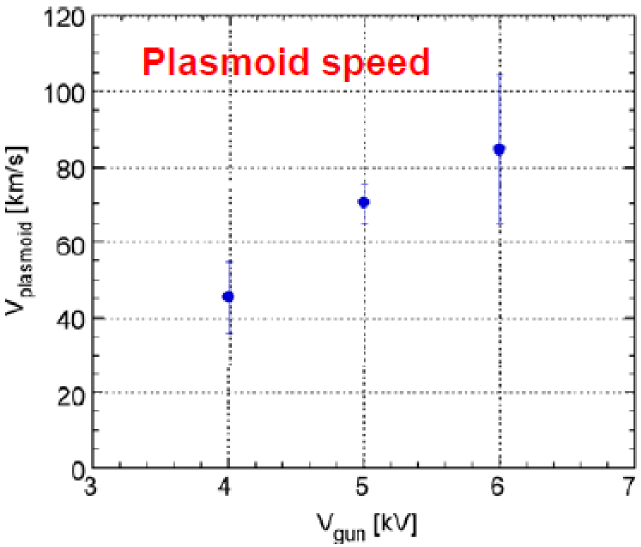

Dependence of CT velocity on V_{gan}
(Y. Kikuchi et al. , Univ. Hyogo)

CT Injector installed in TPE-RX
(vertical injection)

CT Speed required for injection to RELAX：
～35 km/s

Rapid decrease in double-filter SXR temperature is observed at the relaxation event

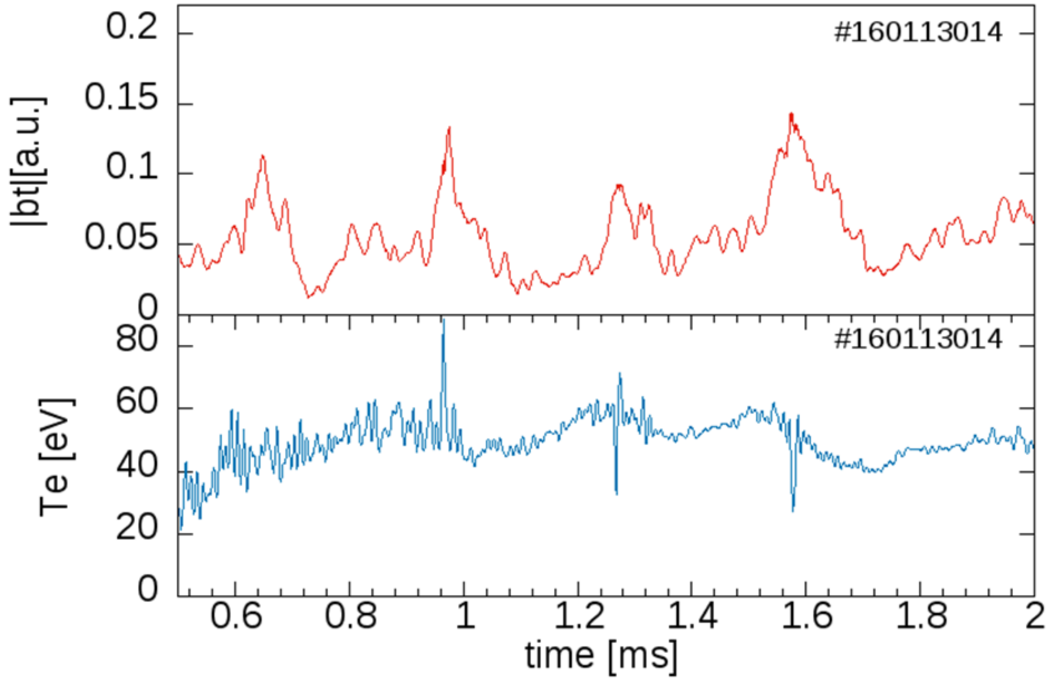

- **Discrete relaxation event is observed during the flat-topped current phase.**
- **The electron temperature estimated from double-filtered SXR signals decreases as a resut of relaxation.**

Rapid decrease is also observed in Thomson temperature at the relaxation event

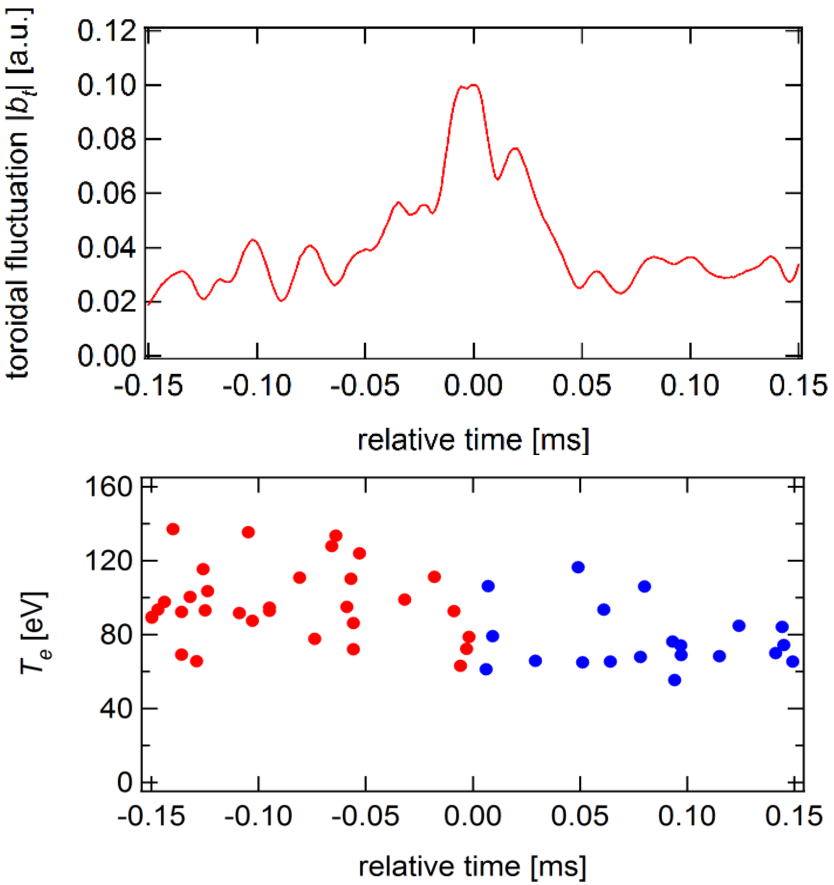

- **Shot-by-shot single point data are replotted with respect to the discrete relaxation event over almost identical shotsand events**
- **The trend is that Thomson temperature is lowered after the relaxation event**

The temperature decrease may be related to magnetic reconnection associated with MHD relaxation cycle

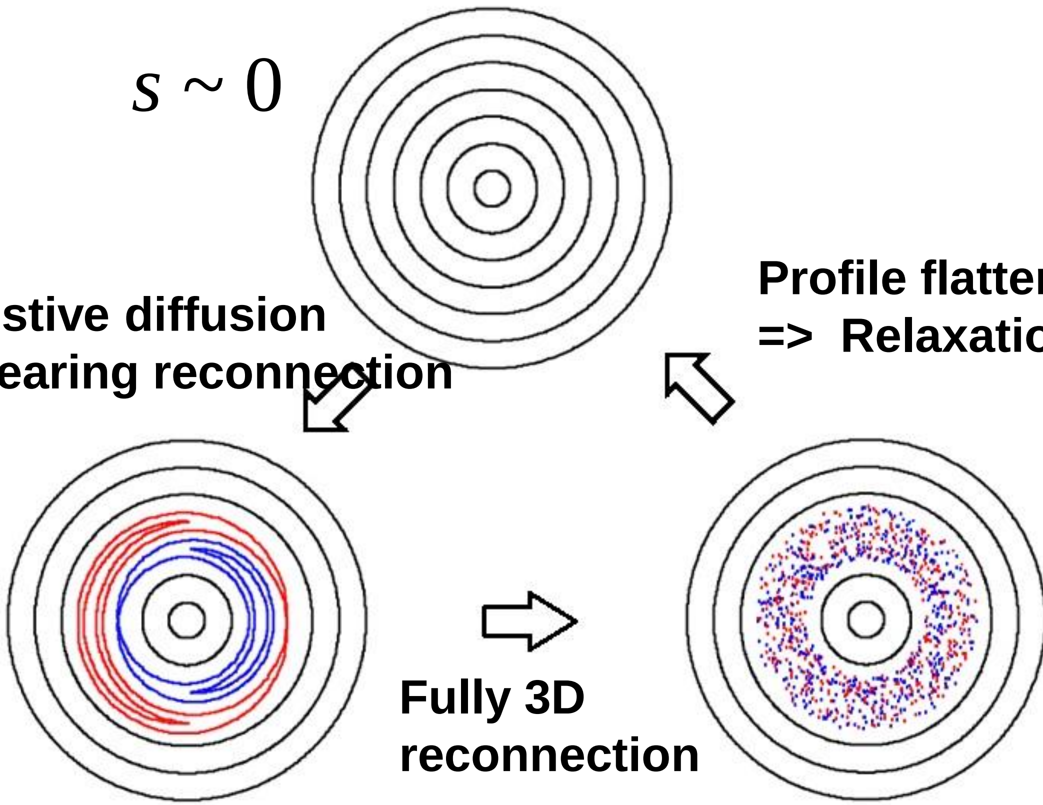

Chirikov parameter

$$s = \frac{1}{2}\frac{\Delta_{mn} + \Delta_{m'n'}}{|r_{mn} - r_{m'n'}|}$$

Question associated with CTinjection:

- How does the reconnection evolve after the CT injection?

Summary

- As the performance of RELAX plasmas is improved, we are in a good position to verify bootstrap current in a low-A RFP.
- Further efforts to obtain higher temperature and higher density are in progress for high-beta plasmas with improved performance.
  - Electron temperature=>high current, PPCD?
  - Electron density=>fast gas puffing.
- A scenario for achieving high performance QSH with good controllability is required.
- Evaluation of CT injection (for helicity injection) in current rise phase to save poloidal flux is in progress.

Thank you for your attention.

3-D MHD simulation study on formation process of helical RFP state in low-A configuration

Simulation Model

- nonlinear MHD
- resistive
- compressible

Governing equations

$$\frac{\partial \rho}{\partial t} = -\nabla \cdot (\rho \boldsymbol{u}),$$

$$\rho \frac{\partial \boldsymbol{u}}{\partial t} = -\boldsymbol{\omega} \times \boldsymbol{u} - \rho \nabla (\frac{u^2}{2}) - \nabla p + \boldsymbol{j} \times \boldsymbol{B} + \frac{4}{3} \nabla [\nu \rho (\nabla \cdot \boldsymbol{u})] - \nabla \times (\nu \rho \boldsymbol{\omega}),$$

$$\frac{\partial p}{\partial t} = -\nabla \cdot (p \boldsymbol{u}) - (\gamma - 1) p \nabla \cdot \boldsymbol{u} + (\gamma - 1) \left[\nu \rho \omega^2 + \frac{4}{3} \nu \rho (\nabla \cdot \boldsymbol{u})^2 + \eta j^2 \right]$$

$$\frac{\partial \boldsymbol{B}}{\partial t} = -\nabla \times \boldsymbol{E},$$

$$\boldsymbol{E} = -\boldsymbol{u} \times \boldsymbol{B} + \eta \boldsymbol{j},$$

$$\mu_0 \boldsymbol{j} = \nabla \times \boldsymbol{B},$$

$$\boldsymbol{\omega} = \nabla \times \boldsymbol{u}.$$

Numerical geometry

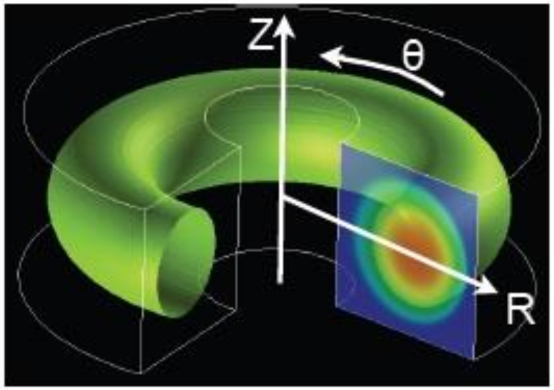

$\eta = 1 \times 10^{-5}$

$\nu = 8 \times 10^{-4}$

$P = \nu / \eta = 80$

$H = (\eta \nu)^{-1/2} = 10^5$

grid size

$(N_R \times N_Z \times N_\theta) = (112 \times 112 \times 128)$

MHD solver:
MIPS : MHD Infrastructure for Plasma Simulation
(Y. Todo et al., Plasma Fusion Res. 5 (2010) S2062.)

Nonlinear evolution of iso-pressure contours to the helical RFP state

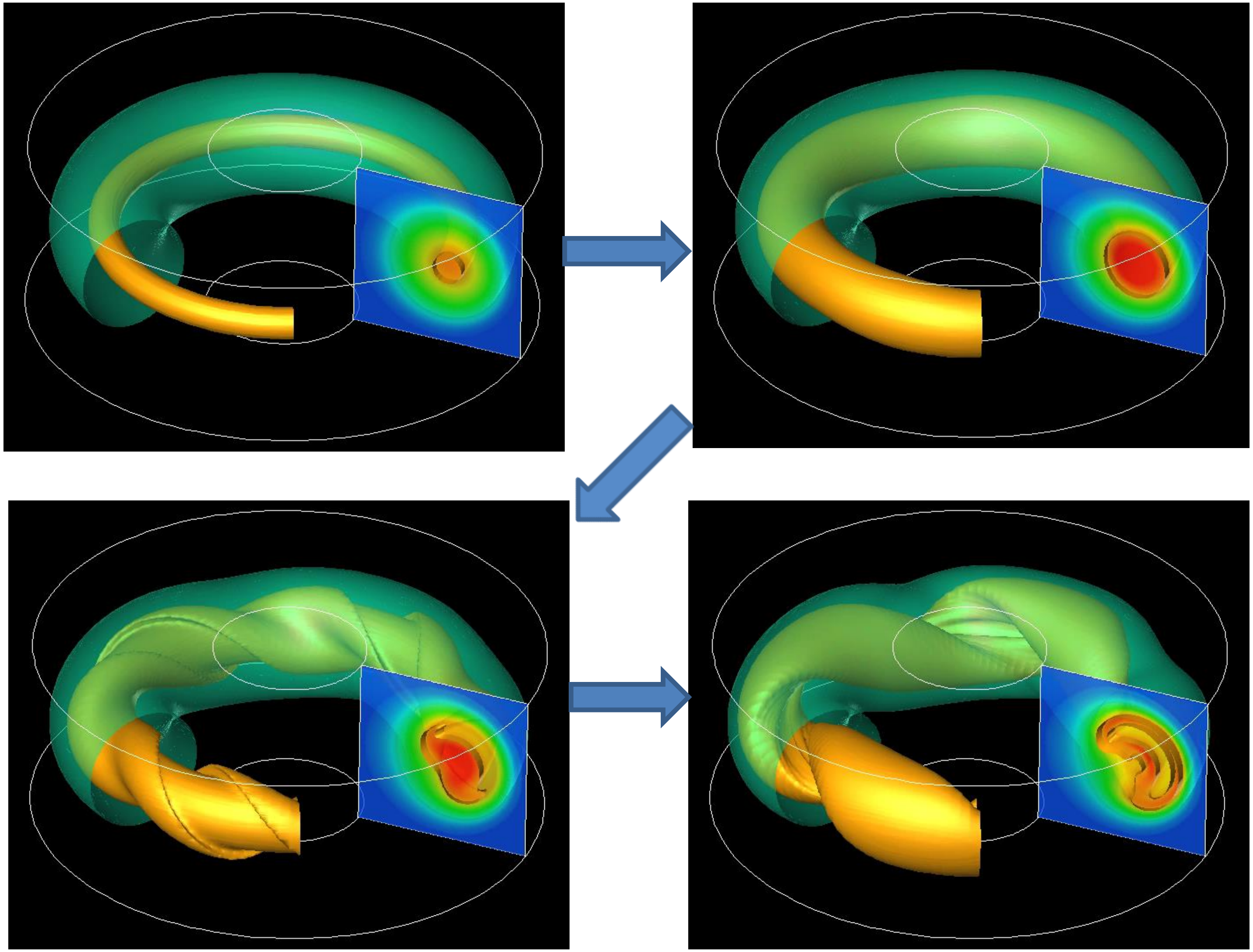

(Mizuguchi et al., PPCF 2012)